Geophys. J. R. astr. Soc. (1984) **79**, 513–538

Intraplate lithosphere deformation and the strength of the lithosphere

N. J. Kusznir and R. G. Park *Department of Geology, University of Keele, Keele, Staffordshire ST5 5BG*

Received 1984 March 19; in original form 1983 October 4

Summary. The intraplate deformation of continental lithosphere in response to applied stress has been investigated using a mathematical model which incorporates the elastic, ductile and brittle response of lithosphere material. Ductile deformation is assumed to be controlled in the crust by dislocation creep in quartz, and in the mantle by dislocation creep and plasticity in olivine. Brittle failure is predicted using modified Griffith theory. A fundamental feature of the model is the redistribution of stress within the lithosphere following stress release by both ductile and brittle deformation. This redistribution produces high levels of stress in the middle or lower crust immediately above the elastic-ductile or brittle-ductile transition.

Lithosphere deformation is shown to be critically dependent on the temperature structure of which surface heat flow is a convenient indicator. For higher geothermal gradients, the release of stress in the lower lithosphere by ductile deformation is more rapid and complete and results in large stress levels in the upper lithosphere. For sufficiently large applied stresses or steep geothermal gradients, the stress levels in the upper and middle crust will cause complete fracture of the upper lithosphere. *Whole lithosphere failure* (WLF) then results, by continued brittle and ductile deformation, causing geologically significant strains.

The critical value of applied stress required to give WLF has been calculated for both tensional and compressional deformation as a function of surface heat flow. The predicted lithosphere bulk strength is then compared with expected levels of intraplate stress arising from plate boundary forces and isostatically compensated loads, which are thought to give net stress levels in the continental lithosphere in the range +0.25 to −0.25 kB. Using these expected maximum stress levels, the model predicts significant extensional deformation in regions of moderate heat flow with $q > c.\ 60\,\mathrm{mW\,m^{-2}}$ (e.g. Central Europe) as well as for areas of high heat flow like the Basin-and-Range Province. Significant compressional deformation is predicted for areas of high heat flow with $q > c.\ 75\,\mathrm{mW\,m^{-2}}$ but only for restricted conditions of stress combination. These results are in good agreement with

the observed rather widespread incidence of extensional intraplate deformation and the restricted occurrence of compressional deformation which may be confined to areas of unusually high heat flow or weak crust.

The model may also be used to calculate the depth of the brittle-ductile transition which is shown to become shallower with increase in heat flow, in good agreement with seismic evidence.

1 Introduction

The lithosphere plate as originally conceived by the early proponents of the plate tectonics model was regarded as part of a relatively strong layer which exhibited no significant internal lateral distortion over time periods of the order of tens or hundreds of Ma. Evidence for lack of distortion was the exactness of fit of the severed passive continental margins of the Atlantic (Bullard, Everett & Smith 1965) and the general applicability to relative plate motions of the concept of tectonics on a sphere (McKenzie & Parker 1967 and Le Pichon 1968). Significant lithosphere deformation was thought to be confined to plate boundaries.

This view is now regarded as oversimplified in the light of more recent discoveries of the importance of deformation within the interior of continental plates – for example, the large areas of recent deformation in Central Asia attributed by Molnar & Tapponnier (1975) to the India–Asia collision, and the many cases of extensional tectonics associated with the formation of graben, rifts and sedimentary basins found within all the major continental plates. Studies of extensional basins stimulated in part by the conceptual model of McKenzie (1978) envisage local crustal extensions of 100 per cent or more over time periods of the order of tens of Ma. Structural studies of the currently active extensional zone of the Basin-and-Range Province of the western USA (e.g. Zoback, Anderson & Thompson 1981 and Wernicke *et al.* 1982) have revealed previously unrecognized large horizontal strains of the order of 100 per cent over *c.* 30 Ma. Compressional intraplate tectonics in contrast appears to be much less common – many examples being probably due to the reversal of movements on previous extensional fault systems (*cf.* Zeigler 1982). The best known examples of active intra-plate compressional tectonics are in Central Asia north of the Himalayas plate boundary (see Molnar & Tapponnier 1975).

In contrast to the behaviour of continental plates, oceanic intraplate deformation appears to be neither pervasive nor extensive and is generally confined to brittle deformation in the upper crust associated with insignificant strains or to lithosphere flexure associated with sediment or sea-mount loading (e.g. Bodine, Steckler & Watts 1981).

The magnitude of the stresses involved in intraplate deformation must clearly be large enough to promote frequent though localized extensional failure in continental lithosphere but too small to promote compressional failure except under unusual circumstances. This paper is an attempt to quantify these stresses and to investigate the conditions required for significant lithosphere failure.

The sources and distribution of tectonic stress in the lithosphere have been investigated by Forsyth & Uyeda (1975), Turcotte & Oxburgh (1976) and Richardson, Solomon & Sleep (1976). The most important sources responsible for significant tectonic stress arise from plate boundary forces and from isostatically compensated loads (Bott & Kusznir 1984). The sources and estimated stress levels are summarized in Table 1 and are discussed in greater detail later. The average stress levels within present continental plates arising from these sources seem likely to lie within the range -0.25 to $+0.25$ kB if distributed over the whole lithosphere plate. However measured and calculated stresses in the upper and middle parts of the crust are much larger – Heard (1976) suggests a maximum value for the stress

Table 1. Contributions to tectonic stress.

Source of Tectonic Stress	Expected Stress Magnitude distributed over lithosphere	
	in OCEANIC† LITHOSPHERE	in CONTINENTAL× LITHOSPHERE
Plate Boundary Forces		
(a) Ridge Push	0.2-0.3 kb (compression)	0.1-0.15 kb (compression)
(b) Slab Pull*	0-0.5 kb (mainly tension)	0-0.25 kb (mainly tension)
(c) Subduction Suction	0-0.3 kb (tension)	0-0.15 kb (tension)
Compensated Load Forces		
(a) Continental Margin	0 (but up to 0.2 kb compression)	0.1 kb (tension)
(b) Plateau Uplift	-	0-0.3 kb (tension)

* Slab Pull Stress is the net resultant of slab pull, subduction resistance and collision resistance forces.
† For oceanic lithosphere – 80 km thick.
× For continental lithosphere – 150 km thick.

difference of *c.* 3 kB. Uniaxial compressive fracture strengths of common rocks are in the range 1–4 kB and tensile strengths approximately 1/8 of these values. The comparatively low levels of expected intraplate stress must therefore be reconciled with levels of upper lithosphere stress large enough to cause significant though localized crustal failure. The explanation for this apparent discrepancy lies in the ductile nature of the lower part of the lithosphere which causes redistribution of a stress applied to the whole lithosphere and its amplification in the more brittle upper part of the lithosphere.

This process of *stress amplification* has been investigated mathematically for various types of lithosphere (Kusznir & Bott 1977; Bott & Kusznir 1979; Mithen 1982; Kusznir & Park 1982). The instantaneous response of the lithosphere to the application of an applied external stress will take the form of elastic deformation with strains of the order of 0.01 per cent. Creep in the lower ductile lithosphere causes stress decay and associated stress redistribution and amplification in the upper lithosphere, leading to an increase in the elastic strains there. If the amplified stress in the upper lithosphere is sufficiently large, fracture will occur in the topmost brittle part of the lithosphere. Associated stress release further increases the stress levels in the remaining competent elastic core (Fig. 1). For sufficiently high levels of applied stress, the whole of the upper brittle lithosphere may fracture, leading to stress release and transfer to the lower ductile lithosphere where further creep and upward transfer then occurs. Thus a cyclic process of upper lithosphere fracture and lower lithosphere creep is established which results ultimately in complete failure throughout the competent elastic core when the stress levels everywhere exceed the failure strength (Fig. 1). This development is defined as *whole lithosphere failure* (WLF) after which extensive lithosphere deformation with large horizontal strains will take place.

The temperature structure of the lithosphere, because of its effect on lithosphere rheology, is critically important in controlling not only the time taken for complete failure to occur, but also the rate at which subsequent deformation takes place (Kuznir & Park 1982). This may be illustrated for example by the relative weakness of lithosphere with a Basin-and-Range type geotherm compared with lithosphere with a typical continental shield

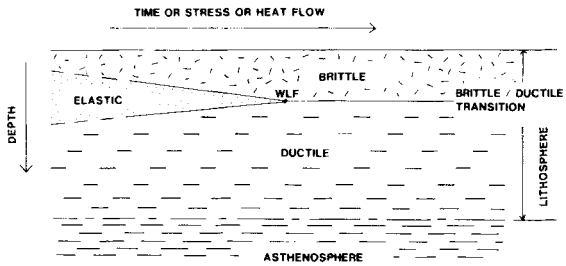

Figure 1. A diagrammatic representation of the regions of brittle, elastic and ductile behaviour in visco-elastic lithosphere under an applied lateral stress. With increase in time, given a large enough applied stress, the elastic core will be reduced to zero as the regions of brittle and ductile deformation extend downwards and upwards respectively. The point in depth at which this occurs corresponds to the brittle/ductile transition. *Whole lithosphere failure* (WLF) occurs when the elastic layer disappears. An increase in heat flow has a similar effect to increasing stress.

geotherm. Using the mathematical model described below, the critical values of applied stress may be found which will cause WLF and significant lithosphere deformation, with geologically appropriate strain rates in the range 10^{-14}–10^{-15}, for a series of different geotherms (represented by their surface heat flow values).

The main purpose of this paper is to establish a relationship between critical applied stress and heat flow which may then be applied to specific geological situations (e.g. Basin-and-Range Province, Western Europe, Central Asia) where a comparison can be made between expected and theoretical stress values.

2 The lithosphere deformation model

The mathematical model examines the elastic, ductile and brittle response of the lithosphere to lateral applied stress. Fundamental to the model is the conservation of the total horizontal force arising from that stress. The model calculates the stress transfer caused by brittle failure in the upper lithosphere and ductile creep in the lower lithosphere and the resulting strain distribution. An initial horizontal stress σ_0 is applied uniformly to the lithosphere in the x-axis direction. The perpendicular horizontal axis is labelled y and the vertical axis z (measured positive downwards).

Conservation of the horizontal force arising from the applied stress gives the equation:

$$\int_0^L \sigma_x \, dz = \text{constant}$$

where σ_x is the horizontal stress in the lithosphere and L is the lithosphere thickness. Differentiation of this equation with respect to time gives:

$$\int_0^L \dot{\sigma}_x \, dz = 0.$$

The assumption that the various layers of the lithosphere are welded together and that the lithosphere undergoes a uniform horizontal strain with depth gives the equation:

$$\frac{d\epsilon_x}{dz} = 0$$

or differentiating with respect to time

$$\frac{d\dot{\epsilon}_x}{dz} = 0.$$

The lithosphere is assumed to behave as a Maxwell viscoelastic material in which stress is also relieved by brittle deformation. Stress and strain within the lithosphere are linked by the equation

$$\epsilon_x = \frac{1}{E}(\sigma_x - \sigma_x^0) - \frac{\nu}{E}(\sigma_y - \sigma_y^0) - \frac{\nu}{E}(\sigma_z - \sigma_z^0) + \epsilon_x^v$$

where ϵ_x is the total horizontal strain, σ_x is the total stress in the x-direction, σ_x^0 is the initial stress, ϵ_x^v is the ductile creep in the x-direction, E is Young's modulus and ν is Poisson's ratio. Initial stresses σ_x^0, σ_z^0 and σ_y^0 are used for modelling stress release by brittle fracture. Similar equations exist for strains ϵ_y and ϵ_z.

Plane strain in the y-direction gives the additional equation $\epsilon_y = 0$, while the vertical stress σ_z arising from the applied stress is zero, i.e. $\sigma_z = 0$. Manipulation and integration of the above equations gives the final equations for the temporal and spatial variations of σ_x and σ_y

$$\dot{\sigma}_x = \int_0^t \left(\frac{1}{L} \int_0^L k\dot{\epsilon}_V \, dz - k\dot{\epsilon}_V \right) dt' - \frac{1}{L} \int_0^L \sigma_x^0 \cdot dz + \sigma_x^0$$

$$\dot{\sigma}_y = \int_0^t \left[\nu\dot{\sigma}_x - E\frac{(2\sigma_y - \sigma_x)}{6\eta} \right] dt' + \sigma_y^0 - \nu\sigma_x^0$$

where $k = E/(1 - \nu^2)$.

The derivation of these equations is described in greater detail by Kusznir (1982).

Ductile deformation within the lower and middle lithosphere is assumed to be accomodated by non-Newtonian power-law creep. For the mantle, ductile creep in olivine is assumed to provide the dominant creep mechanism. Following the experimental work of Kohlstedt & Goetze (1974), Goetze (1978) has suggested that dislocation (power-law) creep provides the dominant creep mechanism for olivine except at high deviatoric stresses ($\tau > 2$ kB). For higher levels of stress Goetze suggests that a Dorn law is more applicable. Post (1977) has shown that a dislocation creep mechanism is also applicable for (wet) dunite. Bodine *et al.* (1981), drawing on the olivine and dunite creep laws of Goetze and Post and on their own modelling of oceanic lithosphere flexure, propose the following relationship between creep rate, stress and temperature for dislocation and Dorn law creep in the mantle:

dislocation creep

$$\dot{\epsilon} = 7 \times 10^{10} \exp\left(\frac{-53\,030.3}{T}\right)(\sigma_1 - \sigma_3)^3 \text{ s}^{-1} \qquad \text{for } (\sigma_1 - \sigma_3) < 2 \text{ kB}$$

Dorn law

$$\dot{\epsilon} = 5.7 \times 10^{11} \exp\left[\frac{-55\,555.6}{T}\left(1 - \frac{(\sigma_1 - \sigma_3)}{85}\right)^2\right] \text{s}^{-1} \qquad \text{for } (\sigma_1 - \sigma_3) > 2 \text{ kB}$$

where $(\sigma_1 - \sigma_3)$ is in kB (1 kB = 100 MPa).

For the continental crust, dislocation creep in quartz is assumed to be the dominant mechanism controlling creep deformation. As with olivine, the amount of water strongly controls the creep rates; creep rates being greater for greater water content. The ductility of crust controlled by creep in quartz will consequently be dependent on the crustal water content and on the amount of quartz, both of which will decrease with depth. The upper crust is assumed to deform according to a wet quartz rheology with 50 per cent quartz composition while the lower crust, on the assumption of a granulite facies composition is assumed to deform according to a dry quartz model with 10 per cent quartz. The above model for the crustal rheology is of course a gross oversimplification and certain qualifications relating particularly to the lower crust should be pointed out: (1) the lower crust in certain situations may be wet; (2) creep in plagioclase may be important; and (3) cataclastic flow may be a significant mechanism. The creep rates used for wet and dry quartz are as follows and are based on the experimental work of Koch, Christie & George (1980):

wet quartz:

$$\dot{\epsilon} = 4.36 \exp\left(\frac{-19\,332.08}{T}\right)(\sigma_1 - \sigma_3)^{2.44}\ \mathrm{s}^{-1}$$

dry quartz:

$$\dot{\epsilon} = 0.126 \exp\left(\frac{-18\,244.65}{T}\right)(\sigma_1 - \sigma_3)^{2.86}\ \mathrm{s}^{-1}$$

where $(\sigma_1 - \sigma_3)$ is in kB.

Brittle deformation within the lithosphere has been predicted by the use of Griffith's theory (1924) as modified by McClintock & Walsh (1962) and described by Jaeger & Cook (1971). Three failure domains have been used – tensional failure, open crack compressional and closed crack compressional. The physical parameters within the modified Griffith theory which control failure are tensile strength, T_0; the frictional coefficient, μ and the critical stress, σ_{gc}, required to close the Griffith crack. Of these parameters T_0 and μ have the greatest influence on brittle failure.

Estimates of tensile strength, T_0, from laboratory experiments for crystalline rocks (Jaeger & Cook 1971; Brace 1964) lie predominantly in the range 0.1–0.4 kB. A value of 0.2 kB has been generally used in the calculation of this paper although in Section 4 and Fig. 8 the effect of a lower value is investigated.

Values of the coefficient of friction, μ, estimated from laboratory experiments (Jaeger & Cook 1971; Byerlee 1978) lie predominantly in the range 0.5–1.0. Tests on fault gouge clay material give a much lower value for μ of the order of 0.1 (Wang & Mao 1979). However such low μ material would only be present in the top few kilometres of the crust giving way with increase in depth and metamorphism to cataclasite material (Sibson 1983). Heat flow observations over the San Andreas Fault (Lachenbruch & Sass 1980) which show the absence of any significant heat flow anomaly have been interpreted to suggest a low faulting stress and consequently a low value of μ. The determination of μ by this technique is however extremely indirect and the reliability of the estimated value uncertain. The value of μ should, according to the Anderson theory of faulting, be related to the angle between a fault plane and the maximum principal stress, σ_1. Turcotte (1983) has used a dip of 35° for the Wind River Thrust to give a value of $\mu = 0.35$. However values of the angle between the fault plane and σ_1 commonly range for normal and thrust faults between 20° and 35° corresponding to a range of μ of 1.2–0.35. $\mu = 0.5$ may be taken as a representative estimate and this value has been generally used in the calculations of this paper. In addition, the

effects of $\mu = 1$ have been investigated in Section 4 and Fig. 8 in order to include the higher laboratory estimates of μ, and as will be seen make little difference to the results.

The stress required to close the Griffith cracks, σ_{gc} has been reported by Murrell (1965) to be $-4.19\ T_0$ which gives an estimate for σ_{gc} of the order of 0.8 kB. However estimates of the crack closure stress from core samples from the Michigan basin (Wang & Simmons 1978) give a higher value of 1.45 kB. An intermediate value of 1.0 kB has been used in this paper.

Failure is dependent on stresses σ_x and σ_z. The stress σ_y, being the intermediate stress, is not required in the 2-D Griffith–McClintock and Walsh formulation. At failure the stress σ_x is returned to the failure envelope (the stress σ_z is simply lithostatic).

The model has been tested against a more elaborate 3-D plane strain finite element model and the results are identical. The formulation described above, however, provides for greater spatial and temporal resolution.

The temperature dependence of the ductile component of the lithosphere deformation suggests that the lithosphere temperature is a critical parameter. Continental lithosphere temperature structure has been calculated using the lithosphere temperature model of Pollack & Chapman (1977). The lithosphere temperature field is identified by the surface heat flow.

3 Application of the model to continental lithosphere

3.1 THE DISTRIBUTION OF STRESS WITH DEPTH

The mathematical model of lithosphere deformation described above has been applied primarily to the deformation of continental lithosphere. The response of continental shield lithosphere with a heat flow of $q = 45$ mW m^{-2} and thickness 150 km subjected to an initial tensional stress of 0.2 kB is shown in Fig. 2(a).

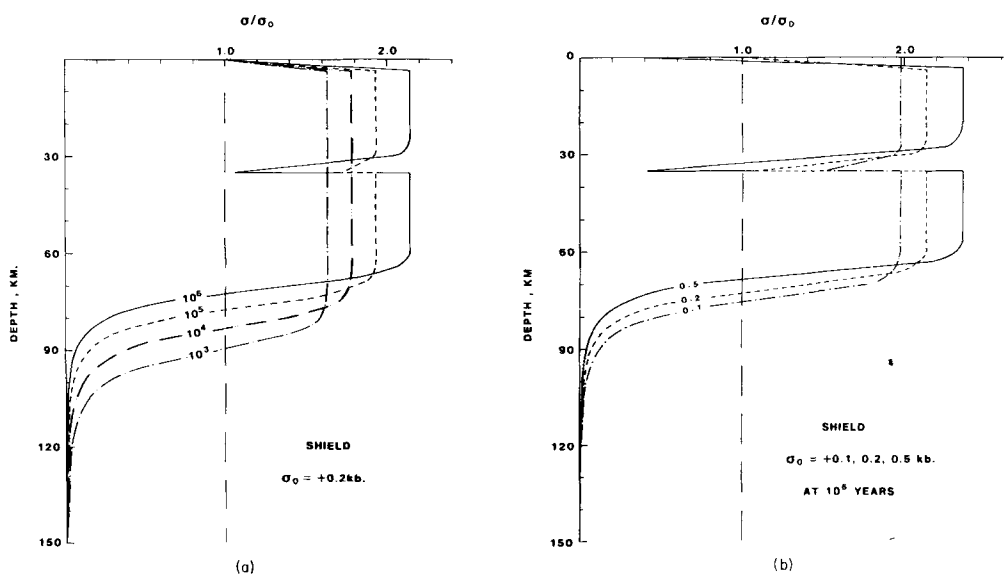

Figure 2. Horizontal stresses within continental shield type lithosphere plotted against depth: (a) at various times following the application of an initial stress $\sigma_0 = +0.2$ kB; (b) at time 10^6 yr after stress application, for initial applied stresses of $\sigma_0 = +0.1, +0.2$ and $+0.5$ kB.

The stress/depth profiles are shown at various times after the application of the stress. As time increases, ductile creep in the lower lithosphere leads to the decay of stress there and its transfer to the upper lithosphere. By 10^6 yr, stress decay in the lower half of the lithosphere is almost complete and the level of stress within the upper lithosphere has been increased by a factor of approximately $\times 2$. The amplification of stress in the upper lithosphere has also resulted in brittle fracture in the topmost lithosphere and the transfer downwards of the released stress. With increase in time, the high ductility zone at the base of the lower crust (with quartz rheology) becomes more apparent.

The stress response of a piece of lithosphere is dependent on the magnitude of the applied stress, since both the brittle and ductile deformation are dependent on it. In Fig. 2(b) stress in continental shield lithosphere is shown at 10^6 yr after the application of various levels of initial stress varying between 0.1 and 0.5 kB. For the greater initial stress values the ductile deformation in the lower lithosphere proceeds more rapidly and greater stress amplification in the upper lithosphere results. This arises primarily from the power-law dependence of strain rate on stress. The low stress region at the base of the continental crust also becomes more apparent for greater levels of applied stress.

The behaviour of lithosphere with a hotter temperature structure is shown in Fig. 3 for Basin-and-Range type lithosphere with $q = 95$ mW m^{-2}. In Fig. 3(a) stress is shown as a function of depth at times 10^3 and 10^4 yr after the application of an initial tensional stress of 0.2 kB. The hotter lithosphere has undergone effectively complete stress decay within the mantle and lowermost crust with resulting stress amplification in the middle crust by a factor of between $\times 8$ and $\times 11$. The large levels of amplified stress in the upper crust have resulted in extensive brittle failure. The stress profiles with depth show two subsidiary stress peaks or discontinuities below a stress minimum at approximately 15 km depth. These subsidiary peaks result from the discontinuities in rheology as composition changes from wet to dry quartz and from dry quartz to olivine respectively.

Fig. 3(b) shows the response of Basin-and-Range continental lithosphere to an applied compressive stress of 0.2 kB. Comparison of the stress profiles for both tensional and

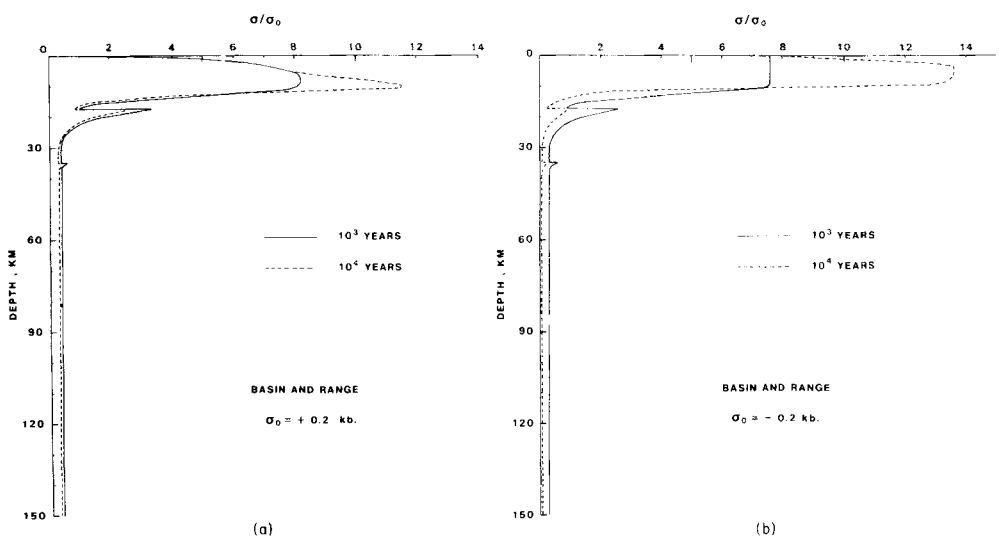

Figure 3. Horizontal stresses within Basin-and-Range type lithosphere plotted against depth at times 10^3 and 10^4 yr after the application of an applied stress: (a) $\sigma_0 = +0.2$ kB; (b) $\sigma_0 = -0.2$ kB.

compressive stresses at 10^3 yr shows that no failure has occurred for the compressive stress, while significant failure in the upper crust has occurred for the tensile case. The tensile stress case has a greater amplified stress showing that a significant contribution to stress amplification can arise in the middle crust due to brittle failure.

In Fig. 3(a) the curve for the tensile applied stress at 10^4 yr shows that the brittle failure envelope has intersected the top of the region in which ductile deformation has occurred, resulting in a sharp stress peak. The elastic core of the lithosphere for this model at this time consequently has ceased to exist with all of the lithosphere experiencing significant brittle or ductile deformation. The lithosphere in this model has consequently suffered *whole lithosphere failure* (WLF). In contrast, the stress profile for compressive applied stress at 10^4 yr (Fig. 3b) shows that WLF has not occurred.

In Fig. 4 the stress/depth profiles for continental shield and Basin-and-Range lithosphere are compared with those of ocean-basin lithosphere with a heat flow of 60 mW m^{-2}. Stresses are shown at 10^3 yr after the application of an applied stress of 0.2 kB. The rheology of the oceanic lithosphere is assumed to be controlled by olivine and the initial thickness of the oceanic lithosphere, over which the stress is applied, is 80 km. The oceanic lithosphere has undergone a similar amount of stress amplification to the continental shield lithosphere and has also suffered little brittle deformation compared with the Basin-and-Range model. While the oceanic lithosphere model has a higher heat flow than the continental shield model, it contains a greater proportion of lithosphere with the stronger olivine rheology.

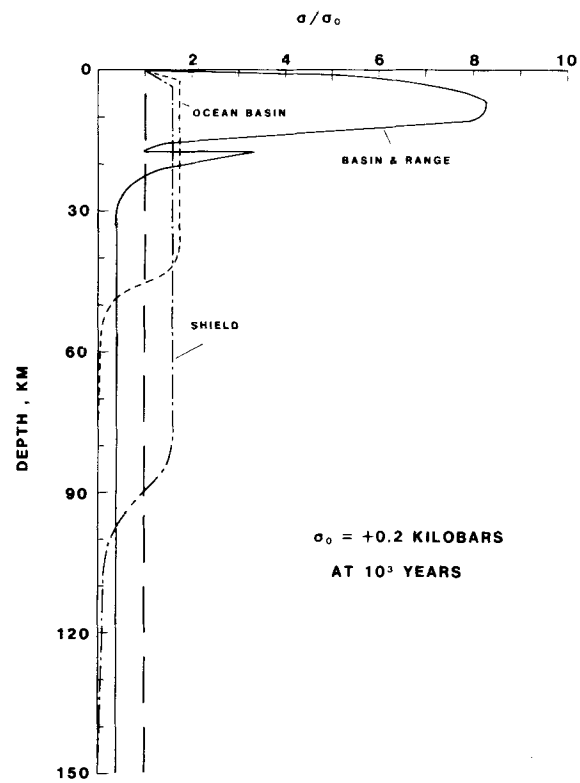

Figure 4. A comparison of stress as a function of depth for shield, Basin-and-Range and ocean-basin lithosphere at time 10^3 yr after the application of an initial stress $\sigma_0 = +0.2$ kB.

3.2 THE DEVELOPMENT OF LITHOSPHERE DEFORMATION

The ductile and brittle deformation of the lithosphere in response to the applied lateral stress will result in horizontal strains which for lithosphere undergoing WLF will become geologically significant. In Fig. 5(a), horizontal strain ϵ_x in the lithosphere, expressed as a percentage, is plotted as a function of time for various lithosphere models. At 1 Ma the strain of the hotter Basin-and-Range model subjected to 0.2 kB tension is approaching 100 per cent. In contrast, the strains in the cooler continental shield and oceanic basin models, at 10^6 yr, are of the order of 0.01 per cent. Such strains would not be geologically observable. Also shown in Fig. 5(a) is the strain–time curve for Basin-and-Range lithosphere subjected to an applied compressive stress of 0.2 kB. The strain in this model at 10^6 yr is only just approaching 1 per cent, and is significantly less than that of the tensile model. The upturn in the curve however suggests that WLF may be about to occur.

The dependence of the horizontal strain within the lithosphere both on the lithosphere temperature structure and on the sign of the applied stress is illustrated in Fig. 5(b) where strain is plotted against time for various models with heat flow values between 40 and 100 mW m^{-2}. The temperature structures were calculated using the Pollack & Chapman (1977) continental lithosphere temperature model. For the tensile applied stress curves, WLF occurs at about 10^3 yr for lithosphere with $q = 80$–100 mW m^{-2}. For cooler lithosphere with $q = 60$ mW m^{-2}, WLF occurs much later at about 10^5 yr. For compressional applied stress, only the curve with $q = 100$ mW m^{-2} shows WLF occurring by 1 Myr.

The dependence of the horizontal strain on the magnitude of the stress is demonstrated in Fig. 6 where strain–time curves are shown for lithosphere with $q = 60$ mW m^{-2} subjected to both tensile and compressive stresses between 0.1 and 0.5 kB. The curves for tensile applied stress of 0.2 and 0.5 kB show WLF by 1 Myr. However, for compression only the 0.5 kB curve shows geologically observable strains by 10^6 yr and strain rates in the geologically significant range.

4 The strength of intraplate lithosphere

In the previous section it has been shown that stress amplification is critical in explaining how the relatively small intraplate stresses available from known sources can overcome the high strength of the upper lithosphere to cause complete failure and high strains of the kind necessary to produce significant intraplate crustal deformation. The critical role of the geotherm in controlling the rate and extent of stress concentration is illustrated by the differences in the strain–time curves for shield and Basin-and-Range lithosphere (Fig. 5a). From Fig. 5(b) it may be deduced that geologically significant strain can be expected from lithosphere with $q > 60$ mW m^{-2} under a tensional applied stress of 0.2 kB but only from very hot lithosphere with $q > 80$ mW m^{-2} under a compressive applied stress of 0.2 kB.

It is clear from the above that for any given value of heat flow there will be a critical threshold value of both tensional and compressive applied stress which will cause *whole lithosphere failure* and thereby initiate large geologically significant strains. Fig. 7(a) summarizes the relationship between this critical stress σ_c and heat flow q indicating the fields in which significant deformation are predicted. The critical stress corresponds to that required to generate *whole lithosphere failure* by 1 Myr when initially applied over lithosphere 150 km thick. This diagram can thus be used to calculate, for a region of continental lithosphere of known heat flow, the critical applied stress necessary to cause significant deformation. The critical stress σ_c is very sensitive to relatively small changes in q in the range 40–80 mW m^{-2}. The strength of the brittle upper lithosphere, and consequently the whole lithosphere is controlled by the value of T_0 and μ used in the Griffith failure criterion.

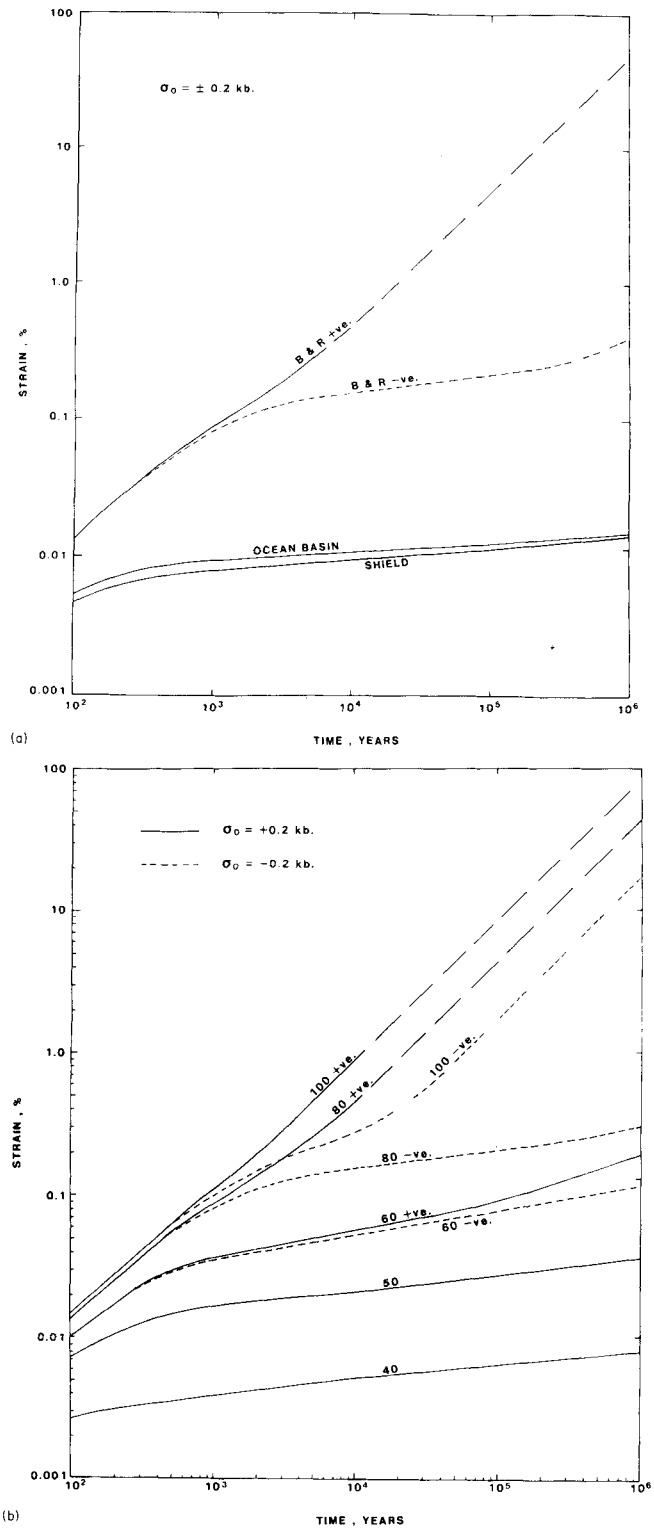

Figure 5. Strain–time curves for an applied stress of ± 0.2 kB: (a) For continental shield, ocean-basin and Basin-and-Range types of lithosphere. Only Basin-and-Range lithosphere shows geologically significant strains. (b) For continental lithosphere with different geothermal structures (characterized by their heat flow values measured in mW m^{-2}).

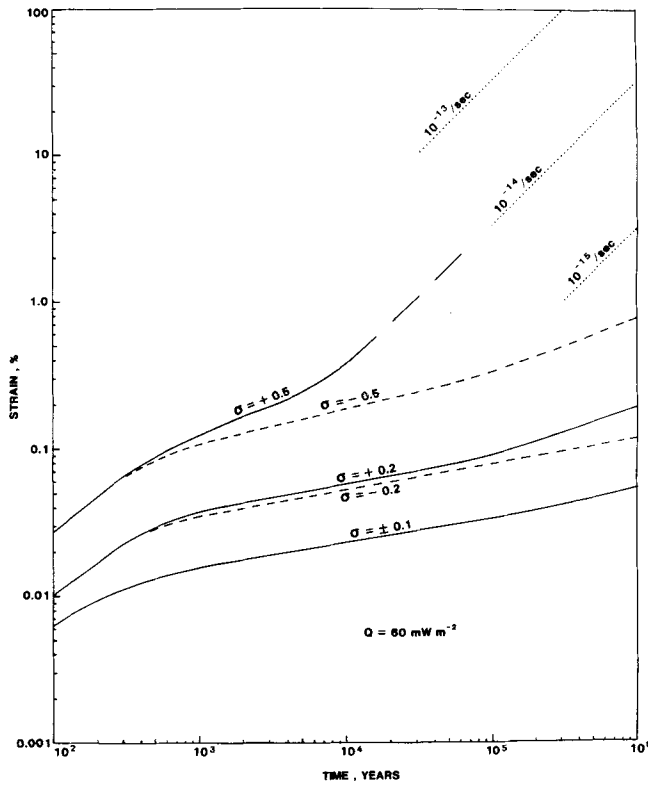

Figure 6. Strain–time curves for continental lithosphere with a geothermal structure corresponding to a heat flow of 60 mW m^{-2}, for applied stresses of ± 0.1, ± 0.2 and ± 0.5 kB. Strain-rate gradients in the geologically important range 10^{-13}–10^{-15} are shown for comparison.

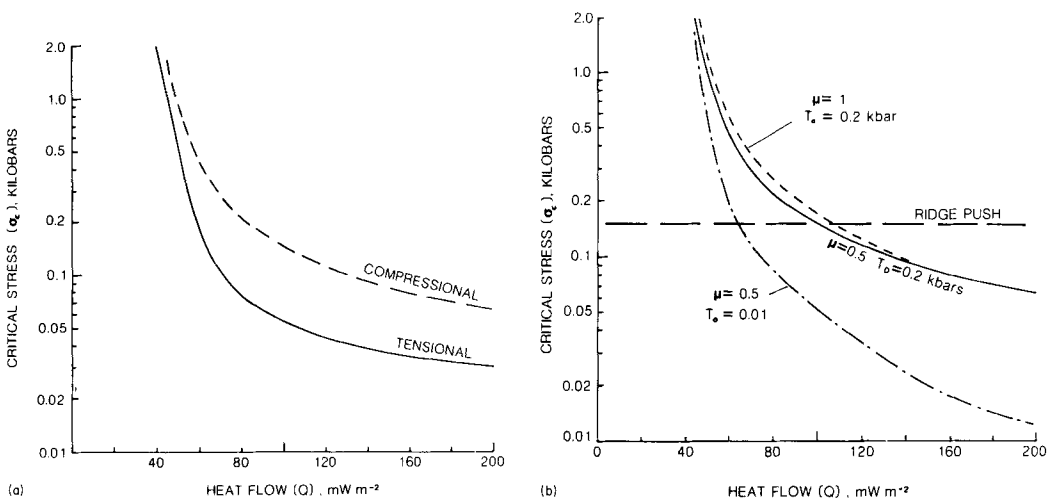

Figure 7. Curves showing the critical stress σ_c, (the initial stress applied over the whole lithosphere required to produce *whole lithosphere failure*) versus lithosphere heat flow q. (a) For both tensile and compressive lithosphere failure. The region above the curve represents the field where WLF occurs leading to significant geological deformation. (b) For compressional failure shown for various values of the parameters controlling brittle failure: T_0 and μ. The likely value of σ_c arising in continental lithosphere from the ocean ridge push force is shown for comparison.

Consequently the inevitable uncertainty is determining T_0 and μ produce corresponding uncertainties in σ_c. The curves of Fig. 7(a) have been calculated using values $T_0 = 0.2$ kB and $\mu = 0.5$. Weakening the model failure strength by choosing a much lower value of T_0 of 0.01 kB (corresponding to low cohesion within previously fractured lithosphere) has the effect of lowering σ_c significantly, especially at higher heat flow values (Fig. 7b). Changes in the value of the coefficient of friction μ within the probable range limits are less significant. The effect of increasing μ to 1.0, as shown in Fig. 7(b), is to increase the lithosphere strength particularly at lower heat flow values.

5 Expected levels of intraplate stress and a comparison with the strength of the lithosphere

The most important sources of tectonic stress in the lithosphere probably arise from plate boundary forces and from isostatically compensated loads. The plate boundary forces consist of *ridge-push, slab-pull* and *subduction suction.* The *ridge-push* force acts at ocean ridges causing a lateral compressive stress of about 0.2–0.3 kB, distributed over the adjacent oceanic lithosphere plate. The slab-pull force, resulting from the negative buoyancy of the sinking lithosphere, acts on the subducting plate and is opposed by lithosphere collision, bending and subduction resistance forces (see Forsyth & Uyeda 1975). The resulting stress in the subducting lithosphere consequently depends on the age of the subducting lithosphere and the rate of subduction. The resulting stress is expected to be generally tensional and in the range 0–0.5 kB. The precise nature of the suction force (Elsasser 1971; Forsyth & Uyeda 1975) is unclear but it is generally accepted that a tensional stress estimated at *c.* 0.2 kB is exerted in the upper (non-subducting) plate as a result of the subduction process. Like its counterpart the slab-pull force, the subduction suction force will be dependent on the age of the subducting lithosphere, on the rate of subduction, and probably in addition on the angle of dip of the subduction zone. Moving plates are also affected by a *mantle drag* force acting on the base of the lithosphere. However this force is considered to be probably an order of magnitude smaller than the plate boundary forces (Schubert *et al.* 1978; Richardson *et al.* 1976). For oceanic lithosphere, the net effect of the above stresses appears generally to be a net compression (see Richardson *et al.* 1976).

In addition to the above forces, the continental plates are affected by *isostatically compensated load stresses* due to topographic loading, crustal thickness variation and low density compensating mantle. These stresses will be associated both with passive continental margins with an estimated magnitude of *c.* 0.1 kB (Bott & Dean 1972) and with plateau uplifts within continents (*c.* 0.3 kB – Bott & Kusznir 1979). A tensional stress is exerted on the loaded compensated part of the lithosphere and a corresponding compressional stress in the adjacent lithosphere.

The stresses associated with the above forces will persist in lithosphere deforming as a consequence of their action. Such stresses have been called *renewable* stresses by Bott & Kusznir (1984). Such stresses are therefore capable of generating considerable tectonic deformation. In contrast, thermal stresses, membrane stresses and lithosphere flexure stresses, although large in magnitude, are dissipated by ductile and brittle lithosphere deformation and are incapable of generating horizontal lithosphere strains of more than a few per cent. Such stresses have been called *non-renewable* by Bott & Kusznir (1984).

It is important in considering the effect of these stresses to calculate their effect over the appropriate lithosphere thickness. Thus the ridge-push force may be calculated as a compressive stress of 0.3 kB when applied to an 80 km thick oceanic lithosphere but is reduced to 0.15 kB when applied to 150 km thick continental lithosphere. The expected levels of stress, within oceanic and continental lithosphere, arising from the main stress sources described above, are summarized in Table 1.

The likely levels of stress expected within continental plates can be approximated in two dimensions by summing the stresses for the various sources. Thus a continental plate with a ridge on each side would be in net compression throughout but the ridge-push element would be partly offset by a tensional continental margin element given a low net compressive stress of the order of 0.05 kB. A continental plate with a subduction zone on each side on the other hand might be expected to show a net tensional stress of up to

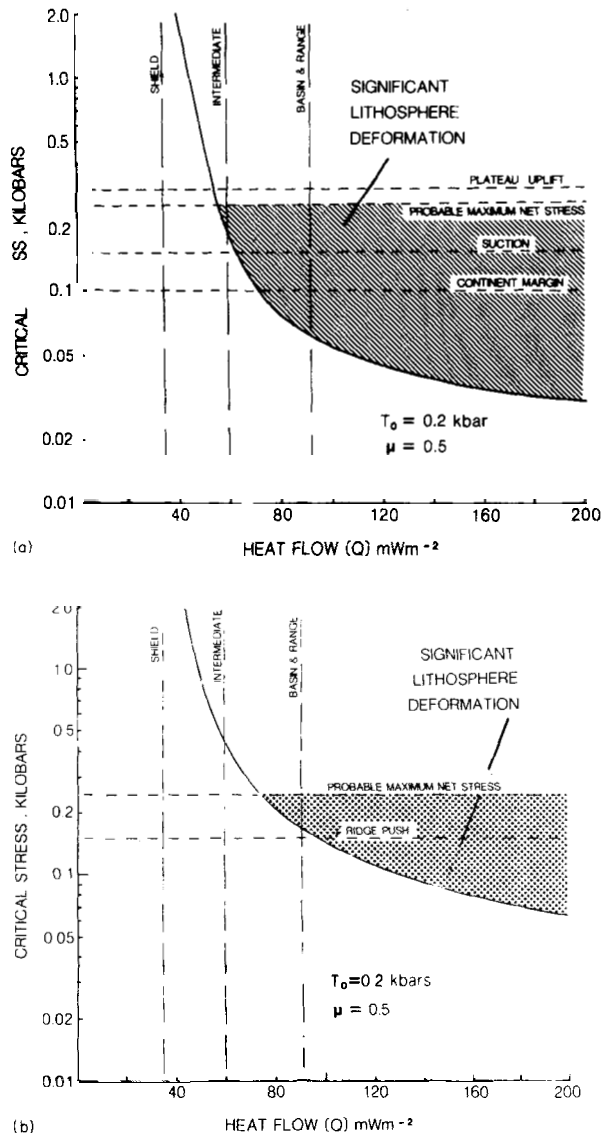

Figure 8. Curves of critical stress σ_c versus lithosphere heat flow, q, for (a) tensional and (b) compressional applied stress compared with possible stress source levels. T_0 = 0.2 kB, μ = 0.5. (a) Field of significant tensional lithosphere deformation compared with estimated stress levels for likely sources of tensional stress (plateau uplift, subduction and continental margin stresses) and for the probable maximum net stress. (b) Field of significant compressional lithosphere deformation compared with the estimated stress level from ocean-ridge push, and for the probable maximum net stress.

c. 0.3 kB (*cf.* the break-up of Pangaea during the Mesozoic). In a more complex example like the present-day northern American plate, the state of stress would be expected to vary from net tensional within the Basin-and-Range plateau uplift to compressional in the eastern part of the continent affected by the mid-Atlantic ridge-push.

Considering only the sources of stress already discussed, it seems likely that the stress levels within present continental plates are within the range −0.25 to +0.25 kB – although locally these levels could be exceeded due to other contributions from non-renewable stresses (e.g. thermal or membrane stresses).

The expected levels of continental intraplate stress can be compared with the strength of the lithosphere predicted by the lithosphere deformation model. Fig. 8(a) indicates the field of likely extensional lithosphere deformation in relation to the theoretical stress levels associated with the main sources of tensional intraplate stress (plateau uplift, subduction suction and continental margin effects). In practice these tensional stresses would be partly offset by compressional stresses and it is unlikely that in present-day continental lithosphere a net (renewable) tensional stress exceeding 0.25 kB exists. In the case of compressional deformation (Fig. 8b) the likely maximum net stress level may be of the same order but would only be achieved in a piece of continental lithosphere affected by adjacent plateau uplift.

In summary, therefore, the lithosphere deformation model predicts significant extensional deformation in continental regions with heat flow values $q \geqslant c.\ 60\ \mathrm{mW\,m^{-2}}$ given a favourable combination of stress sources, and significant compressional deformation with $q \geqslant c.\ 75\ \mathrm{mW\,m^{-2}}$ under rather restricted conditions of stress combination. For more usual levels of compressive stress (*cf.* the ridge push estimate of 0.15 kB) failure would only occur in very hot or very weak lithosphere (*cf.* the lower curve of Fig. 7b).

6 The depth of the brittle-ductile transition

The application of stress to the lithosphere results in ductile deformation in the lower lithosphere and in brittle fracture in the upper lithosphere. If *whole lithosphere failure* has not occurred, the regions of brittle and ductile deformation are separated by a region of mechanically competent lithosphere which has suffered only elastic deformation (Fig. 1). However for increased values of applied stress, or with the progress of time as the stress amplification effect occurs, the regions of brittle and ductile deformation extend downwards and upwards respectively until they meet annihilating the elastic core of the lithosphere. This is the point at which WLF occurs. This process can be seen occurring in Fig. 3(a) and is represented schematically in Fig. 1. The position at which the regions of brittle and ductile deformation meet corresponds to the brittle-ductile transition.

The depth of the brittle-ductile transition can be determined from the deformational model and is dependent on the lithosphere temperature structure. In Fig. 9(a) the depth of the brittle-ductile transition is shown as a function of lithosphere heat flow. Separate curves are shown for tensile and compressional applied stress. The depth of the brittle-ductile transition can be seen to decrease with increase in heat flow. Tensile deformation can be seen to produce a slightly deeper brittle-ductile transition than compressional. For the tensile applied stress model, for heat flows less than approximately $60\ \mathrm{mW\,m^{-2}}$, two brittle ductile transitions are predicted by the model – one in the quartz rheology crust and the other in the olivine rheology mantle.

The curves shown in Fig. 9(a) correspond to models for which WLF occurs at 1 Myr after the application of the applied stress. The levels of stress required to produce such deformation are greater for lower levels of heat flow (see Fig. 7a). The curves are shown dashed for

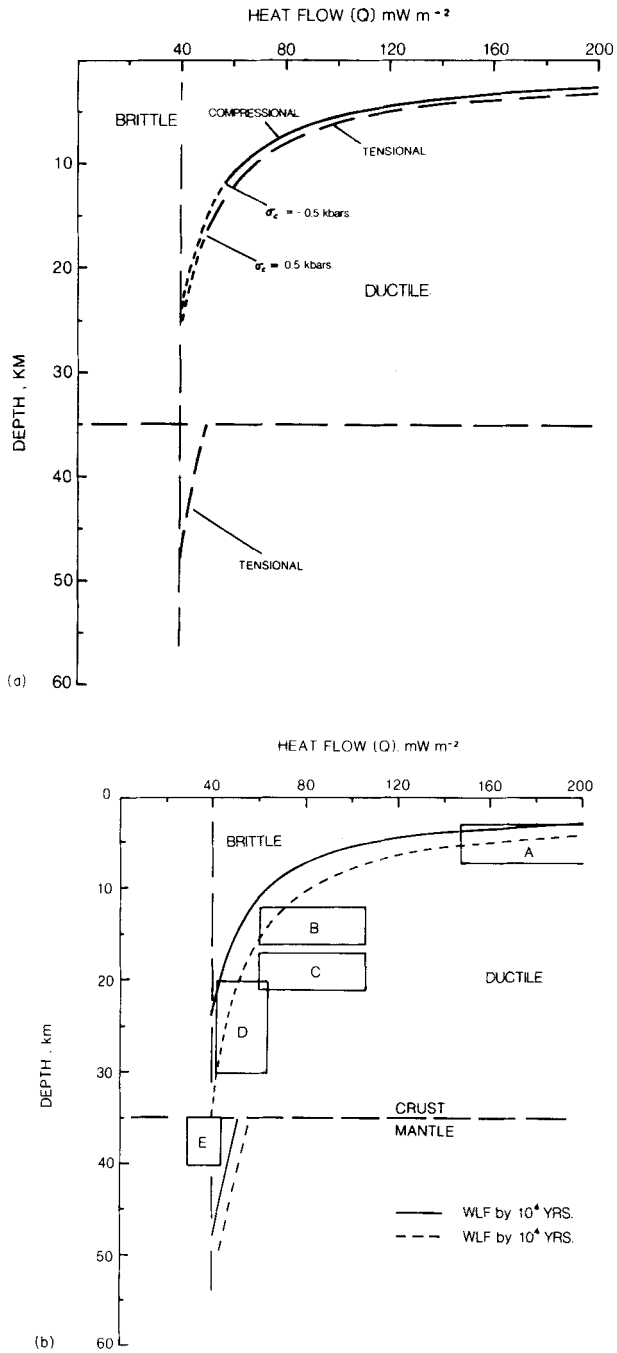

Figure 9. Plots of the calculated depth of the brittle-ductile transition against lithosphere heat flow. (a) Curves for compressive (solid line) and tensional (dashed line) deformation. The deformation rate corresponds to WLF by 1 Ma. The curves are shown dotted for deformation requiring an unrealistically large critical stress σ_c greater than ± 0.5 kB. (b) A comparison of the calculated brittle-ductile transition depth against observations of the brittle-ductile transition depths based on seismic evidence adapted from Sibson (1982). Seismic data areas are: (A) Geysirs and Clearlake Highlands. (B) Central California and Coso Range. (C) Wasatch Front. (D) Eastern US and Canada. (E) Sierra Nevada. Theoretical curves are shown for deformation rates corresponding to WLF by 10^4 (dashed line) and 10^6 yr (solid line).

models in which an applied stress greater than ±0.5 kB is required. Such large levels of stress are unlikely to be applied to the lithosphere (see Section 5) except in exceptional circumstances. Average strain rates of the models shown in Fig. 9 decrease with increasing heat flow ranging between approximately 0.1 and 1 per cent Ma^{-1} corresponding to strain rates of 10^{-16}–10^{-15} s^{-1}.

In Fig. 9(b) a composite curve for both tensile and compressive applied stress is shown for the relationship between brittle-ductile transition depth and heat flow. Also shown is a composite curve for tensile and compressional deformation for models in which WLF occurs at 10^4 yr after the initial application of stress. The latter models require greater levels of applied stress than the former. Average strain rates for this model vary between 100 and 10 per cent Ma^{-1}, decreasing with increase in heat flow. It can be seen that decreasing the time to WLF (and therefore increasing the strain rate) has the effect of deepening the brittle-ductile transition.

Also shown in Fig. 9(b) are estimates of the depth of the brittle-ductile transition depth as a function of heat flow, based on observations of the depth distribution of some continental earthquakes. The data shown are taken from Sibson (1982) and the brittle-ductile transition depth is estimated by assuming that it corresponds to the deepest observed seismic foci. The focal mechanisms correspond to extensional, thrust and strike-slip faulting. While the agreement with the transition depth predicted by the model is not perfect, the general dependence on heat flow is similar. The observed data would appear to correspond better to the faster strain-rate model. However the slower strain-rate curve could be made to fit the observed data by using a weaker brittle strength or a stiffer rheology for the crust.

7 Geological applications

7.1 INTRA-PLATE EXTENSION

Significant continental intra-plate extension appears to be confined to continental rift zones and rift-related basins. There is no general agreement among students of continental rift zones as to a simple mechanism for the initiation and evolution of such structures although crustal extension is now generally considered to be a major factor in their development. Active rift zones appear to be characterized by crustal thinning and by the formation of a 'low-velocity pillow' of hotter less dense asthenospheric material within the mantle part of the lithosphere (Illies 1970; Hermance 1982). There are great differences in the extent and character of magmatism related to rift zones. For example the total volume of volcanic products in the East African rift (*c.* 500 000 km^3 according to Baker, Mohr & Williams 1972) contrasts with only 5000 km^3 in the Baikal rift (Logatchev & Florensov 1978). Moreover the nature and extent of magmatism and the extent of crustal doming or uplift varies considerably along the length of individual rift systems and from one rift to another.

Some authors believe that many rifts result primarily from thermal anomalies below the lithosphere perhaps aided by favourable stress states in the overlying lithosphere; others believe that lithospheric extension is the primary cause and that thermo-magmatic effects are secondary and result from lithosphere thinning. A third possibility is that both mechanisms have operated and that some (weakly or non-volcanic) rifts are extensional in origin while others are primarily thermal in origin. The various models are discussed in summaries by Neumann & Ramberg (1978) and Mohr (1982). It is apparent from studies of individual rifts that the formation of a depression rather than crustal updoming is the first stage in the development of many rift zones (Mohr 1982) suggesting that the model of hot-spot generated, subsequently rifted, crustal domes (Burke & Dewey 1973) is not universally applicable.

Whether or not a thermal anomaly initiated the extension, the generation of any extensional rift structure must depend at least partly on the regional state of stress within the lithosphere and our model will therefore give estimates of the minimum stress conditions necessary for the initiation of continental rifts under specified thermal conditions, and will thus make some contribution to resolving the above dilemma. We consider the application of our model to five well-documented examples of intra-plate extensional tectonics: the Rhine graben, the Baikal and East African rifts, the North Sea basin, and the Basin-and-Range Province.

7.2 THE RHINE GRABEN

This is part of an extensive central European rift system formed in late Eocene–early Oligocene times with associated volcanic activity and intermittently active until the present day (Illies 1978; Ziegler 1982). According to Illies (1978) and Illies & Greiner (1978) initial subsidence took place in Eocene times, and the climax of tensional rifting in the late Eocene–early Oligocene coincided with the culmination of Alpine compression; this is seen as a reflection of the same stress field. Since mid-Pliocene times the stress axes have changed to a NW–SE σ_1 direction producing mainly sinistral strike-slip motion along the rift. Total extension across the rift is about 10 per cent according to Zeigler (1982). The present heat flow of 107 ± 35 mW m^{-2} in the upper Rhine graben compares with a value of 73 ± 20 for the Hercynian fold belts to the north and east (see Morgan 1982).

If we assume that the heat flow of 73 mW m^{-2} (similar to other areas of Hercynian orogenic crust) is representative of thermal conditions at the time of initiation of the rift, then according to Fig. 8(a) a tensional stress of just under 0.1 kB would be sufficient to initiate the rifting. An extensional stress of this magnitude could perhaps be envisaged in mid-Tertiary times if the effect of subduction at the Pacific end of the Eurasian plate more than offset the compressional element arising from the mid-Atlantic ridge (*cf.* Bott 1982). The effect of the north–south compression resulting from the Alpine collision, as suggested by Illies (1978), may have been an important contributory factor in raising the differential stress to the critical level.

However the initiation of the rift may be related to regional late Cretaceous–Palaeocene extension preceding the development of the Greenland–Norway spreading axis. The rift follows in part an old line of structural weakness, the Mjøsa–Mediterranean shear zone, which may also have played an important role in its initiation.

7.3 THE BAIKAL RIFT

This is situated in the central part of the Eurasian plate, about 3000 km north of the Himalayan suture zone. This 2500–3000 km long active rift has no obvious connection with any other rift system or with a plate boundary. The earliest volcanic activity associated with the rift is late Cretaceous in age but the bulk of the rift-related fissure eruption took place in Miocene to early Pliocene times (Logatchev *et al.* 1978; Logatchev & Florensov 1978). A figure of 10 km extension (*c.* 9 per cent) is given by these authors.

The heat flow in the rift is 97 ± 22 compared with 45 ± 10 mW m^{-2} in the Siberian platform to the west (Precambrian shield) and 55 ± 10 mW m^{-2} for the Caledonian fold belt to the SE (Morgan 1982). The rift is situated at the centre of a large uplifted region above a zone of abnormally low seismic velocity and presumably higher temperature in the upper mantle.

If the initiation of the extension preceded the thermal anomaly, we have to consider the likely extensional stress required for failure in crust with a heat flow of *c.* 55 mW m^{-2}. According to Fig. 8(a) a stress of *c.* 0.25 kB would be required which is about the limit of what might be expected by adding the effects of Pacific subduction suction and the Eurasian continental margin. The likely time of initiation of the rift coincides with the late Cretaceous to early Eocene collision between India and the Lhasa block (Allegre *et al.* 1984) which, by imposing a N–S compression on the central part of the Eurasian plate, may have been a contributory factor.

7.4 THE EAST AFRICAN OR KENYA RIFT

This is part of a rift system extending for about 3500 km through eastern Africa to connect with the Red Sea–Gulf of Aden rift, which has been an actively spreading plate boundary since about upper Oligocene times. Baker & Wohlenberg (1971) give a figure of 10 km extension for the Kenya rift since the Miocene (i.e. about 20 per cent extension). The rift is situated on a large regional uplift associated with a negative Bouguer anomaly with a width of more than 1000 km indicating the presence of a large low-density asthenosphere pillow (Fairhead 1976). The course of the rift network is strongly influenced by younger Precambrian tectonic trends and avoids the older Tanzanian craton. The average heat flow within the rift is 105 ± 51 mW m^{-2} compared with 52 ± 17 mW m^{-2} for the flank regions (Morgan 1982).

As Bott (1982) has pointed out, the African rift system appears to have developed within the continental part of a plate under general compressive stress arising from the ridge-push effect on each side. This is confirmed by compressional fault-plane solutions of earthquakes outside the rift zone (Fairhead & Stuart 1982). The initiation of the rift in Miocene times is therefore likely to be related to local extensional stress arising from the thermally induced plateau uplift. Assuming that the present flank heat flow approximates to the regional value over the thermal anomaly before rifting, a tensional stress of over 0.3 kB would be required for complete failure (Fig. 8b), near the upper limit of what might be expected. However the rift is continuous with the active spreading rift system in the Red Sea–Gulf of Aden through Ethiopia. The progressively more alkaline trend of the volcanicity southwards from the active spreading rift (Harris 1969) is associated with a progressively decreasing rate of widening southwards (McKenzie, Davies & Molnar 1970; Mohr 1982) suggesting a contribution to the extensional stress field from a wedging effect related to the plate boundary.

7.5 THE NORTH SEA BASIN

This may be taken as an example of the type of sedimentary basin considered in the model developed by McKenzie (1978) which envisages very rapid extension, with lithosphere stretching and thinning, followed by the upwelling of warm asthenosphere generating a thermal anomaly which subsequently cooled. The main extensional faulting phase in the North Sea lasted from mid-Jurassic to early Cretaceous times (about 60 Ma) with strains in the range 10–55 per cent (Wood & Barton 1983). The total extension estimated by considering the change in crustal thickness however, is up to 80 per cent (Wood & Barton 1983) and much of this extension relates to the initial phase of rifting which occurred in the Triassic (Zeigler 1982).

The early Tertiary onset of seafloor spreading in the Norwegian–Greenland sea caused the North Sea rift to become inactive, and the subsequent history of the basin may be

interpreted as the effect of continued regional depression resulting from the cooling and subsequent disappearance of an anomalous upper mantle rift pillow of Jurassic age (*cf.* Bott 1982b; Zeigler 1982).

In order to apply the model to the North Sea basin, we must consider the conditions prevailing in Triassic times with lithosphere of normal thickness but unknown thermal gradient. The initial generation of the North Sea basin was part of a process of rifting which affected the whole of Pangaea prior to its break-up and has been discussed by Froidevaux & Schubert (1975), Bott (1982b) and Bott & Kusznir (1984). Tensile stresses might have arisen mainly from subduction suction effects around much of the contemporary continental margin providing a net stress of over 0.2 kB. According to Fig. 8(a) this would be sufficient for extensional rifting given intermediate heat flow values of *c.* 60 mW m^{-2} or over – similar to those in present-day Palaeozoic orogenic crust of western Europe.

7.6 THE BASIN-AND-RANGE PROVINCE

This is a large currently active extensional region situated near the western margin of the American plate, mainly in Nevada and Arizona. According to Zoback *et al.* (1981) the current phase of extensional deformation commenced about 10 Ma ago and has resulted in extensional strains of 15–30 per cent (an average strain rate of *c.* 10^{-15} s^{-1}). However this recent phase followed a more prolonged extensional phase in the period 30–10 Ma leading to much larger extensional strains of the order of 50–100 per cent or even more. Total extensions of as much as 300 per cent have been proposed by Wernicke (1981). The earlier extensional phase was initiated between 20 and 30 Ma ago in association with basaltic volcanism, and has been ascribed to back-arc processes related to subduction of the Farallon plate below the Pacific continental margin (Zoback *et al.* 1981). This tectonic setting suggests that a thermal anomaly would have accompanied the earlier rifting phase and that substantial structural and thermal weakening of the lithosphere may have taken place before the modern rifting phase began.

If the present heat flow of 92 ± 33 mW m^{-2} (see also the figure of 100 ± 15 for the related Rio Grande rift) (Table 2) is indicative of the thermal conditions accompanying the initiation of the modern rifting phase, Fig. 8(a) indicates that a very low tensional stress (*c.* 0.06 kB) would be sufficient to produce rifting. The heat flow in the flanking Colorado plateau is 60 mW m^{-2} (Chapman 1983). If the concentration of extensional effects in the Basin-and-Range Province resulted from a greater mid-Tertiary heating there compared with the Colorado plateau (*cf.* Morgan 1983) the heat flow at the time of initiation of the rifting was presumably somewhere between 60 and 90 mW m^{-2}. If we assume an initial heat flow of 70 mW m^{-2}, an extensional stress of 0.1 kB would be sufficient for failure according to Fig. 8(a). This stress level is lower than the likely tensional stress arising either from the plateau uplift, or from the suction force derived from subduction of the Farallon plate. A larger stress would produce more rapid extension.

7.7 DISCUSSION

These five examples of extensional deformation, four currently active and one inactive, were initiated at different times ranging from Triassic to Miocene and show extensions in the range 10–80 per cent over time periods of 10–100 Ma. The generally rather small extensions quoted yield low average strain rates of *c.* 10^{-16} s^{-1}, or 10^{-15} s^{-1} in the case of the Basin-and-Range Province (*cf.* Fig. 6) compared with typical plate boundary strain rates of *c.* 10^{-14} s^{-1}. The possibility that many rifts may be preceded by (relatively long?) periods

of crustal depression and basin formation (*cf.* Mohr 1982) before 'active' rifting develops suggests that the period of initiation of a rift may be measurable in terms of tens of Ma rather than Ma but that after active rifting commences the rate of deformation presumably increases. It is noteworthy that the extension rate for the hot and more 'evolved' Basin-and-Range Province is an order of magnitude greater than those estimated for the other examples. The strain–time curve for 0.2 kB tension with a heat flow of 60 mW m^{-2} (Fig. 6) might be taken as a representative set of conditions leading to rifting. The curve shows WLF at about 10^5 yr. It is clear by extrapolating this curve that probably several tens of Ma will elapse before a geologically measurable strain of about 1 per cent is reached. An important geological implication of this aspect of our model is that observable evidence of intraplate extension may not appear until many tens of Ma after the imposition of the stress in lithosphere with average heat flow, and that the time of initiation of a rift cannot be simply correlated with the appearance of obvious extensional effects in the geological record.

The heat flow values in the active extensional regions are in the range 92–107 mW m^{-2}. Clearly with such high heat flows our model would predict extensional failure with very low values of extensional stress. However the model can strictly be applied only to the initial stage of rifting – starting from 'normal' lithosphere. Once significant crustal thinning has taken place, both the geometry and the rheology of the lithosphere are changed by the emplacement of warmer asthenosphere material in the lower part of the lithosphere (*cf.* McKenzie 1978) and in many cases by the development of vulcanicity. These changes

Table 2.

Region	Heat Flow, mWm^{-2}	Deformation state
A. Shield		
Superior Province[2]	34 ± 8	no failure
West Australia[2]	39 ± 8	no failure
West Africa (Niger)[2]	20 ± 8	no failure
South India[2]	49 ± 8	no failure
Mean Archaen + older Proterozoic[5]	41 ± 10	no failure
B. Intermediate		
Eastern U.S.A.[2]	57 ± 17	no failure
England and Wales[2]	59 ± 23	no failure
Central Europe (Bohemian massif)[2]	73 ± 18	local failure
Northern China[1]	75 ± 15	local failure
Mean Younger Proterozoic[5]	50 ± 5	-----
Mean Palaeozoic[5]	62 ± 20	-----
C. Thermally active		
Rhine graben[3] (flanks-Rhenish massif)[3]	107 ± 35 (73 ± 20)	extensional failure
Baikal rift[3] (S.E.flank-Older Palaeozoic)[3]	97 ± 22 (55 ± 10)	extensional failure
East African rift[3] (flanks)[3]	105 ± 51 (52 ± 17)	extensional failure
Basin-and-Range Province[2] (E.flank-Colorado plateau)[4]	92 ± 33 (60)	extensional failure

Heat flow data from Pollack & Chapman (1977)[1], Vitorello & Pollack (1980)[2], Morgan (1982[3], 1983[4], 1984[5]).

result in an increased thermal gradient which will in turn cause further structural weakening. The heat flow in an active rift would then be expected to be rather higher than in surrounding areas (e.g. compare the values of 107 ± 35 mW m^{-2} for the south Rhine graben with 73 ± 20 for the bordering Rhenish massif). To make a comparison of the data with the model results, it is necessary to use heat flow values which are representative of the regions *at the time of initiation* of the deformation.

Table 2 summarizes the heat flow data and tectonic status of a number of representative regions divided into (A) *continental shield* (Precambrian cratons), (B) *'intermediate'* (Palaeozoic orogenic crust) and (C) *thermally 'active'* (areas of current or recent rifting and vulcanicity). None of Group A with heat flow values in the range 34–49 mW m^{-2} show signs of significant current deformation (taking 'significant' to mean showing lateral crustal strains of *c.* 1 per cent or more). In group C, high heat flows ($q > 90$ mW m^{-2}) are associated with active volcanicity and extensional rifting. Group B shows a range of heat flow values derived from regions of Palaeozoic orogenic crust which probably correspond to the thermal conditions at the time of initiation of the rifts considered earlier, and which correspond rather closely to the range of 'flanking' heat flow values in the currently active rift areas (52 mW m^{-2} for East Africa to 73 mW m^{-2} for the Rhenish massif).

According to Fig. 8(a), significant extensional deformation should be possible in regions with a heat flow $q >$ *c.* 55 mW m^{-2} provided that favourable stress conditions exist, which is in good agreement with the data of Table 2.

These results suggest that a thermal anomaly is not an essential prerequisite for the formation of an extensional rift, although there are examples (the East African rift) whose initiation by an essentially thermal mechanism is easier to envisage because of the unfavourable stress conditions.

7.8 COMPRESSIONAL FAILURE

Significant intra-plate compressional deformation seems to be uncommon at present. Examples occur in Central Asia north of the Himalayan collision zone between India and Asia. Molnar & Tapponnier (1975) suggest that 200–300 km of crustal shortening and thickening have taken place within the Asian plate as a result of this collision and that much of the compressional deformation is concentrated in narrow fold and thrust belts like those of the Tien Shan and Nan Shan ranges, situated about 1500 km north of the plate suture.

The initial continental contact probably occurred in early to mid-Eocene times but the major effects of the collision appear to date from about the beginning of the Oligocene when large-scale vertical movements indicating crustal thickening and uplift occurred both in Tibet and in the more northerly ranges. At least some of the zones of compressional failure occur along previous (Mesozoic) subduction/collision sutures north of the main Indian suture (*cf.* Mitchell 1981; Allegre *et al.* 1984).

There are insufficient data available either about the heat flow pattern or the tectonic history of the interior of the Asian plate to allow our model to be adequately tested here.

The recently reported very high heat flow figures of 146 mW m^{-2} (Francheteau *et al.* 1984) attributed to high-level igneous intrusions are probably of only local significance. If we take a heat flow value of 75 mW m^{-2} to represent the likely thermal conditions during the initiation of compressional failure in the Oligocene in regions of Hercynian orogenic crust, a stress of -0.25 kB would be required (Fig. 8b) – too large to be attributed to the ridge-push effect alone. Larger compressive stresses could arise from the contribution of the Himalayan–Tibetan plateau uplift on the (presently unjustified) assumption that this preceded the intraplate failure to the north. Alternatively, much higher heat flow might be

associated with residual effects of the older, Mesozoic, subduction zones within the Asian plate.

8 Conclusions

A mathematical model of viscoelastic intraplate lithosphere has been used to investigate lithosphere deformation in response to laterally applied stress and the resulting stress and strain distribution with time. The model incorporates the elastic, ductile and brittle behaviour of the lithosphere and the associated stress transfer resulting from stress release by ductile or brittle failure. Stress decay in the lower lithosphere due to ductile deformation leads to stress amplification in the upper lithosphere. Further amplification arises due to the release of the stress in the uppermost lithosphere by brittle failure and produces large amplified stresses in the middle and lower lithosphere. For sufficiently large levels of applied stress, or sufficiently hot lithosphere, the regions of significant ductile and brittle deformation meet, so destroying the elastic core of the lithosphere. This development has been named *whole lithosphere failure* (WLF) and only after this occurs can geologically significant deformation occur.

The deformation of the lithosphere and the magnitude of the applied stress required for WLF is critically dependent on the thermal structure of the lithosphere as represented by the surface heat flow. Significant, geologically observable, strains of *c.* 1 per cent or more may be produced through WLF over times of *c.* 1 Ma by an applied stress of +0.2 kB in lithosphere with an average heat flow ($q = 60$ mW m^{-2}). Much smaller stress levels are required in hotter lithosphere whereas for cooler shield or ocean-basin lithosphere WLF will not occur except for unrealistically high stress levels.

The magnitude of the applied stress required for WLF is much larger for compressive stress than for tensional. The critical level of applied tensional stress for lithosphere with an average heat flow of 60 mW m^{-2} is just under 0.2 kB. In contrast the critical compressive stress is 0.45 kB. These values are significantly lowered by using a much lower value of the failure strength T_0. For hotter lithosphere (e.g. Basin-and-Range Province) with $q = c.\ 90$ mW m^{-2}, the critical tensional stress is 0.065 kB and the critical compressive stress is 0.17 kB.

The main sources of intraplate stress arising from plate boundary forces and isostatically compensated loads are thought to give likely average net stress levels in the continental lithosphere in the range +0.25 to −0.25 kB. Using these expected maximum stress levels, the model predicts significant extensional deformation in regions with $q \geqslant c.\ 60$ mW m^{-2} and significant compressional deformation for $q \geqslant c.\ 75$ mW m^{-2} (under rather restricted conditions of stress combination). Thus extensional failure is predicted for areas of moderate heat flow (e.g. Central Europe, northern China) as well as for areas of high heat flow like the Basin-and-Range Province, whereas compressional failure is predicted only in areas of rather high heat flow. This is in good agreement with the observed rather widespread occurrence of extensional intraplate deformation and suggests that the much rarer compressional deformation may be restricted to regions of anomalously high heat flow or weak crust.

The model has also been used to calculate the depth of the brittle-ductile transition which is shown to decrease with increase in heat flow. This relationship may be tested against seismic evidence of the brittle-ductile transition depth. Comparison shows generally good agreement, although the seismic evidence shows a consistently deeper brittle-ductile transition depth than the model.

A deeper brittle-ductile transition in the model could be achieved by either using a weaker

brittle failure criterion or a stronger rheology in the middle and lower crust. If the tensile and compressive strengths of the lithosphere in Sections 5 and 7 are of the right order, a combination of a weaker brittle failure criterion together with a stronger rheology would be required to satisfy the seismic brittle-ductile transition data.

In the above model, we have assumed for convenience that the lower crustal rheology is controlled by the deformation of dry quartz (whose rheology is well known). It is possible, however, that quartz is not present in sufficient quantity in the lower crust to form the rock matrix and control the ductile deformation. If so, plagioclase is likely to be the dominant mineral controlling the deformation and, while little is known about its rheology, it will be significantly stronger than quartz. Moreover the predominant deformation mechanisms in the lower crust may well be cataclastic flow, especially in lithosphere with lower heat flow values. There is at present insufficient information available to assess the effect of these factors on the model predictions.

References

Allègre, C. J. *et al.*, 1984. Structure and evolution of the Himalaya-Tibet orogenic belt, *Nature*, **307**, 17–22.

Baker, B. H., Mohr, P. A. & Williams, L. A. J., 1972. Geology of the eastern rift system of Africa, *Spec. Pap. geol. Soc. Am. 136*, **67** pp.

Baker, B. H. & Wohlenberg, J., 1971. Structure and evolution of the Kenya rift valley, *Nature*, **229**, 538–542.

Bodine, J. H., Steckler, M. S. & Watts, A. B., 1981. Observations of flexure and the rheology of the oceanic lithosphere, *J. geophys. Res.*, **86**, 3695–3707.

Bott, M. H. P., 1982a. The mechanism of continental splitting, *Tectonophys.*, **81**, 301–309.

Bott, M. H. P., 1982b. Origin of the lithosphere tension causing basin formation, *Phil. Trans. R. Soc. A*, **305**, 319–324.

Bott, M. H. P. & Dean, D. S., 1972. Stress systems at young continental margins, *Nature*, **235**, 23–25.

Bott, M. H. P. & Kusznir, N. J., 1979. Stress distributions associated with compensated plateau uplift structures with application to the continental splitting mechanism, *Geophys. J. R. astr. Soc.*, **56**, 451–459.

Bott, M. H. P. & Kusznir, N. J., 1984. Origins of tectonic stress in the lithosphere, *Tectonophys.*, **105**, 1–14.

Brace, W. F., 1964. Brittle fracture in rocks, in *State of Stress in the Earth's Crust*, pp. 111–174, ed. Judd, W. R., Elsevier, Amsterdam.

Bullard, E., Everett, J. E. & Smith, A. G., 1965. The fit of the continents around the Atlantic, *Phil. Trans. R. Soc. A*, **258**, 41–51.

Burke, K. & Dewey, J. F., 1973. Plume-generated triple junctions: key indicators in applying plate tectonics to old rocks, *J. Geol.*, **81**, 406–433.

Byerlee, E., 1978. Friction of rocks, *Pure appl. Geophys.*, **116**, 615–626.

Chapman, D. S., 1983. Colorado plateau: thermal-tectonic evolution (abstr.), *Int. U. Geodesy Geophys.*, Hamburg, p. 577.

Elsasser, W. M., 1971. Sea floor spreading as thermal convection, *J. geophys. Res.*, **76**, 1101–1112.

Fairhead, J. D., 1976. The structure of the lithosphere beneath the Eastern Rift, East Africa, deduced from gravity studies, *Tectonophys.*, **30**, 269–298.

Fairhead, J. D. & Stuart, G. W., 1982. The seismicity of the East African rift system and comparison with other continental rifts, in *Continental and Oceanic Rifts*, pp. 41–61, ed. Palmason, G., Geodynamics Series 8, American Geophysics Union.

Forsyth, D. & Uyeda, S., 1975. On the relative importance of the driving forces of plate motion, *Geophys. J. R. astr. Soc.*, **43**, 163–200.

Francheteau, J. *et al.*, 1984. High heat flow in southern Tibet, *Nature*, **307**, 32–36.

Froidevaux, C. & Schubert, G., 1975. Plate motion and structure of the continental asthenosphere: a realistic model of the upper mantle, *J. geophys. Res.*, **80**, 2553–2564.

Goetze, C., 1978. The mechanisms of creep in olivine, *Phil. Trans. R. Soc. A*, **288**, 99–119.

Griffith, A. A., 1924. Theory of rupture, *Proc. first int. Congr. Applied Mechanics*, Delft, A221, 163–198.

Harris, P. G., 1969. Basalt type and African rift valley tectonism, *Tectonophys.*, **8**, 427–436.

Heard, H. C., 1976. Comparison of the flow properties of rocks at crustal conditions, *Phil. Trans. R. Soc. A*, **283**, 173–186.

Hermance, J. F., 1982. Magnetotelluric and geomagnetic deep-sounding studies in rifts and adjacent areas: constraints on physical processes in the crust and upper mantle, in *Continental and Oceanic Rifts*, pp. 169–192, ed. Palmason, G., Geodynamics Series 8, American Geophysics Union.

Illies, J. H., 1970. Graben tectonics as related to crust-mantle interaction, in *Graben Problems*, pp. 3–27, eds Illies, J. H. & Mueller, St.

Illies, J. H., 1978. Two stages Rhinegraben rifting, in *Tectonics and Geophysics of Continental Rifts*, pp. 63–71, eds Ramberg, I. B. & Neumann, E. R., Reidel, Dordrecht.

Illies, J. H. & Greiner, G., 1978. Rhine graben and the Alpine system, *Bull. geol. Soc. Am.*, **89**, 770–782.

Jaeger, J. C. & Cook, N. G. W., 1971. *Fundamentals of Rock Mechanics*, Chapman & Hall, London.

Koch, P. S., Christie, J. M. & George, R. P., 1980. Flow law of 'wet' quartzite in the α-quartz Field, *Trans. Am. geophys. Un.*, **61**, 376.

Kohlstedt, D. L. & Goetze, C., 1974. Low-stress high-temperature creep in olivine single crystals, *J. geophys. Res.*, **79**, 2045–2051.

Kusznir, N. J., 1982. Lithosphere response to externally and internally derived stresses: a viscoelastic stress guide with amplification, *Geophys. J. R. astr. Soc.*, **70**, 399–414.

Kusznir, N. J. & Bott, M. H. P., 1977. Stress concentration in the upper lithosphere caused by underlying viscoelastic creep, *Tectonophys.*, **43**, 247–256.

Kusznir, N. J. & Park, R. G., 1982. Intraplate lithosphere strength and heat flow, *Nature*, **299**, 540–542.

Lachenbruch, A. H. & Sass, J. H., 1980. Heat flow and energetics of the San Andreas Fault zone, *J. geophys. Res.*, **85**, 6185–6222.

Le Pichon, X., 1968. Sea floor spreading and continental drift, *J. geophys. Res.*, **73**, 3661–3697.

Logatchev, N. A. & Florensov, N. A., 1978. The Baikal system of rift valleys, *Tectonophys.*, **45**, 1–13.

Logatchev, N. A., Rogozhina, V. A., Solonenko, V. P. & Zorin, Y. A., 1978. Deep structure and evolution of the Baikal rift zone, in *Tectonics and Geophysics of Continental Rifts*, pp. 49–61, eds Ramberg, I. B. & Neumann, E. R., Reidel, Dordrecht.

McClintock, F. A. & Walsh, J. B., 1962. Friction on Griffith cracks under pressure, *Proc. fourth U.S. Nat. Congr. Applied Mechanics*, pp. 1015–1021.

McKenzie, D., 1978. Some remarks on the development of sedimentary basins, *Earth planet. Sci. Lett.*, **40**, 25–32.

McKenzie, D. P. & Parker, R. L., 1967. The North Pacific: an example of tectonics on a sphere, *Nature*, **216**, 1276–1279.

McKenzie, D. P., Davies, D. & Molnar, P., 1970. Plate tectonics of the Red Sea and East Africa, *Nature*, **226**, 243–248.

Mitchell, A. H. G., 1981. Phaneozoic plate boundaries in mainland SE Asia, the Himalayas and Tibet, *J. geol. Soc. London*, **138**, 109–122.

Mithen, D. P., 1982. Stress amplification in the upper crust and the development of normal faulting, *Tectonophys.*, **83**, 259–273.

Mohr, P., 1982. Musings on continental rifts, in *Continental and Oceanic Rifts*, pp. 293–309, ed. Palmason, G., Geodynamics Series 8, American Geophysics Union.

Molnar, P. & Tapponnier, P., 1975. Cenozoic tectonics of Asia: effects of a continental collision, *Science*, **189**, 419–426.

Morgan, P., 1982. Heat flow in rift zones, in *Continental and Oceanic Rifts*, ed. Palmason, G., Geodynamics Series 8, American Geophysics Union.

Morgan, P., 1983. Uplift of the Colorado plateau and its relationship to volcanism and rifting in the adjacent Basin-and-Range and Rio Grande rift (abstr.), *Int. U. Geodesy Geophys.*, Hamburg, p. 576.

Morgan, P., 1984. The thermal structure and thermal evolution of the Continental Lithosphere, *Phys. Chem. Earth*, in press.

Murrell, S. A. F., 1965. The effect of triaxial stress systems on the strength of rocks at atmospheric temperatures, *Geophys. J. R. astr. Soc.*, **10**, 231–281.

Neumann, E. R. & Ramberg, I. B., 1978. Palaeorifts – concluding remarks, in *Tectonics and Geophysics of Continental Rifts*, pp. 409–424, eds Ramberg, I. B. & Neumann, E. R., Dordrecht.

Pollack, H. N. & Chapman, D. S., 1977. On the regional variation of heat flow, geotherms and lithosphere thickness, *Tectonophys.*, **38**, 279–296.

Post, R. L., 1977. High temperature creep of Mt Burnet Dunite, *Tectonophys.*, **42**, 75–110.

Richardson, R. M., Solomon, S. C. & Sleep, N. H., 1976. Intraplate stress as an indicator of plate tectonic driving forces, *J. geophys. Res.*, **81**, 1847–1856.

Schubert, G., Yuen, D. A., Froidevaux, C., Fleitout, C. & Sourian, M., 1978. Mantle circulation with partial shallow return flow: effects on stresses in oceanic plates and topography of the sea floor, *J. geophys. Res.*, **83,** 745–758.

Sibson, R. H., 1982. Fault zone models, heat flow, and the depth distribution of earthquakes in the continental crust of the United States, *Bull. seism. Soc. Am.*, **72,** 151–163.

Sibson, R. H., 1983. Continental fault structure and the shallow earthquake source, *J. geol. Soc. London,* **140,** 741–767.

Turcotte, D. L., 1983. Mechanisms of crustal deformation, *J. geol. Soc. London,* **140,** 701–724.

Turcotte, D. L. & Oxburgh, E. R., 1976. Stress accumulation in the lithosphere, *Tectonophys.*, **35,** 183–199.

Vitorello, I. & Pollack, H. N., 1980. On the variation of continental heat flow with age and the thermal evolution of continents, *J. geophys. Res.*, **85,** 983–995.

Wang, C. & Mao, N., 1979. Shearing of saturated clays in rock joints at high confining pressures, *Geophys. Res. Lett.*, **6,** 825–828.

Wang, H. F. & Simmons, G., 1978. Microcracks in crystalline rock from 5.3 km depth in the Michigan basin, *J. geophys. Res.*, **83,** 5849–5856.

Wernicke, B., 1981. Low-angle normal faults in the Basin and Range province: nappe tectonics in an extending orogen, *Nature,* **291,** 645–648.

Wernicke, B., Spencer, J. E., Burchfiel, B. C. & Guth, P. L., 1982. Magnitude of crustal extension in the southern Great Basin, *Geology,* **10,** 499–502.

Wood, R. & Barton, P., 1983. Crustal thinning and subsidence in the North Sea, *Nature,* **302,** 134–136.

Zeigler, P. A., 1982. Faulting and graben formation in western and central Europe, *Phil. Trans. R. Soc. A,* **305,** 113–143.

Zoback, M. L., Anderson, R. E. & Thompson, G. A., 1981. Cainozoic evolution of the state of stress and style of tectonism of the Basin and Range province of the western United States, *Phil. Trans. R. Soc. A,* **300,** 407–434.